Mol. BioSyst., 2006, 2, 406 - 410, DOI: 10.1039/b604684c

Retracted article: In-cell protein dynamics

Julie E. Bryant † *

Department of Chemistry, University of North Carolina at Chapel Hill, Chapel Hill, NC 27599, USA

First published on the web 11th July 2006

I, the named author, hereby retract this article. Signed: Julie E. (Bryant) Johnston, September 2007. Retraction endorsed by Dr Sarah Thomas, Managing Editor. Retraction published 18 September 2007.

Julie Bryant earned her BS degree in chemistry from High Point University in 2000. She earned her PhD degree in chemistry at the University of North Carolina at Chapel Hill under the direction of Professor Gary J. Pielak working on the development of in-cell protein NMR. She is currently a post-doctoral fellow at Schering-Plough Research Institute.

Julie Bryant

Introduction

Most protein chemistry is carried out *in vitro* under dilute solution conditions where solute concentrations are typically less than 10 g L^{-1} . These, however, are not the conditions under which most proteins function. Their intracellular environment is a crowded place (Fig. 1), where macromolecular concentrations alone can reach 400 g L^{-1} . [1] Theory predicts that macromolecular crowding can affect a variety of protein properties including their folding, structure, state of aggregation, interactions with other molecules, and stability. [2–5] The question then becomes: does the intracellular environment affect protein characteristics such as structure, stability, and dynamics?

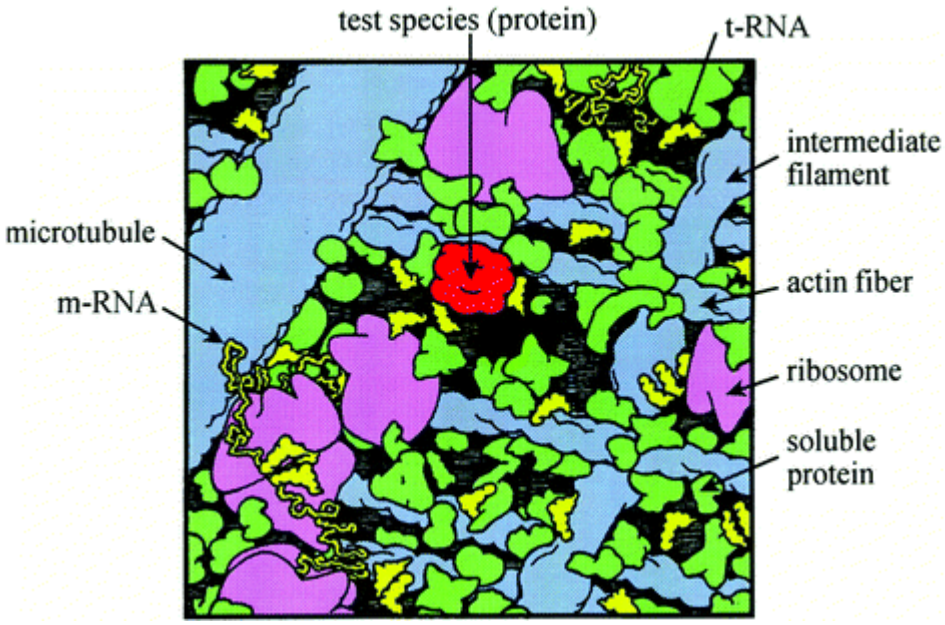

Fig. 1 Depiction of the crowded environment inside a eukaryotic cell magnified approximately a million times. From ref. 28 , reproduced with permission.

To this end, a technique termed 'in-cell NMR' was designed to facilitate the acquisition of atomic-level studies of proteins inside living cells. [6–15] Nuclear magnetic resonance spectroscopy (NMR) allows for the atomic-level, structural investigation of dynamic species, such as proteins, in solution. In-cell NMR allows these data to be obtained for a protein inside living *Escherichia coli*. Initially, in-cell protein NMR was used qualitatively to observe an over-expressed protein of choice in living *E. coli*. We have advanced this technique to yield quantitative biophysical information about protein backbone dynamics inside living cells.

Structure

Apocytochrome b_5 was used for the first quantitative characterization of backbone dynamics using in-cell protein NMR. This protein is the *apo* form of the water-soluble domain of rat microsomal cytochrome b_5 . [16] Due to the lack of a bound heme moiety, the *apo* form of this 98-residue, 11.2 kD electron-transport protein has reduced stability, partial loss of tertiary structure, and highly dynamic regions *in vitro*. [16] Both the *apo* and *holo* forms have been extensively studied *in vitro* under dilute solution conditions, which facilitated comparison of new in-cell data to published dilute solution NMR data.

The reduced stability of apocytochrome b_5 and increased backbone dynamics are caused by the lack of a bound heme moiety. Specifically, apocytochrome b_5 loses structure in the heme-binding region (residues 39–69) and at both termini, leading to a decrease in stability of ~4.3 kcal mol^{-1} . [17,18] In light of the effects of macromolecular crowding, it is possible that the partially folded protein could have a different structure in cells than in dilute solution, specifically a structure resembling that of its more compact *holo*-form. Consistent with this idea, FlgM, a natively disordered protein in dilute solution, gains structure in cells. [3] Therefore, we first had to compare the structure of apocytochrome b_5 in *E. coli* and in dilute solution.

The structure of apocytochrome b_5 was examined inside living cells by inspecting the ^{1}H–^{15}N heteronuclear single quantum coherence (HSQC) spectra obtained using in-cell NMR. The comparison of the HSQC spectrum obtained in *E. coli* with the spectrum of purified apocytochrome b_5 *in vitro* under dilute solution conditions showed no significant changes in cross-peak location, indicating no major changes in apocytochrome b_5 structure under the two different conditions. This congruence also shows that the crowded

intracellular environment is unable to induce native, *holo* structure in apocytochrome b_5. This observation probably means that the structure lost when the heme is removed is "templated" by interactions between the heme and the protein and cannot be stabilized by simply reducing the available volume.

Initial dynamics studies

Because the structure of apocytochrome b_5 was similar under both intracellular and dilute solution conditions, the quantitative investigation of backbone motions in cells could begin without further structural analysis. Understanding protein dynamics is critical to understanding the motions that allow proteins to function. They also provide key information about the ensemble of protein conformations present under a given set of conditions. [19] Protein backbone motion can be quantified by making ^{15}N relaxation measurements using NMR. Typical NMR experiments aimed at quantifying backbone dynamics measure ^{15}N T_1 and T_2 relaxation and the $\{^1\text{H}\}-^{15}\text{N}$ nuclear Overhauser effect (NOE). Both the T_1 and $\{^1\text{H}\}-^{15}\text{N}$ NOE experiments give information about fast motions experienced by individual backbone amide ^{15}N nuclei and are sensitive to motions on the pico- to nanosecond timescales. [20] Both fast and slower motions can be investigated by measuring the T_2 relaxation of the ^{15}N nucleus.

The first in-cell NMR dynamics experiment to be developed measured the steady-state $\{^1\text{H}\}-^{15}\text{N}$ NOE. Once developed, $\{^1\text{H}\}-^{15}\text{N}$ NOE measurements of apocytochrome b_5 both in cells and under dilute solution conditions were obtained for comparison. The results are shown in Fig. 2. [14] Data from both experiments followed similar trends indicating that the intracellular environment of *E. coli* does not drastically alter the fast backbone dynamics of apocytochrome b_5 though small differences were observed. Specifically, many of the NOEs were smaller in cells than in dilute solution.

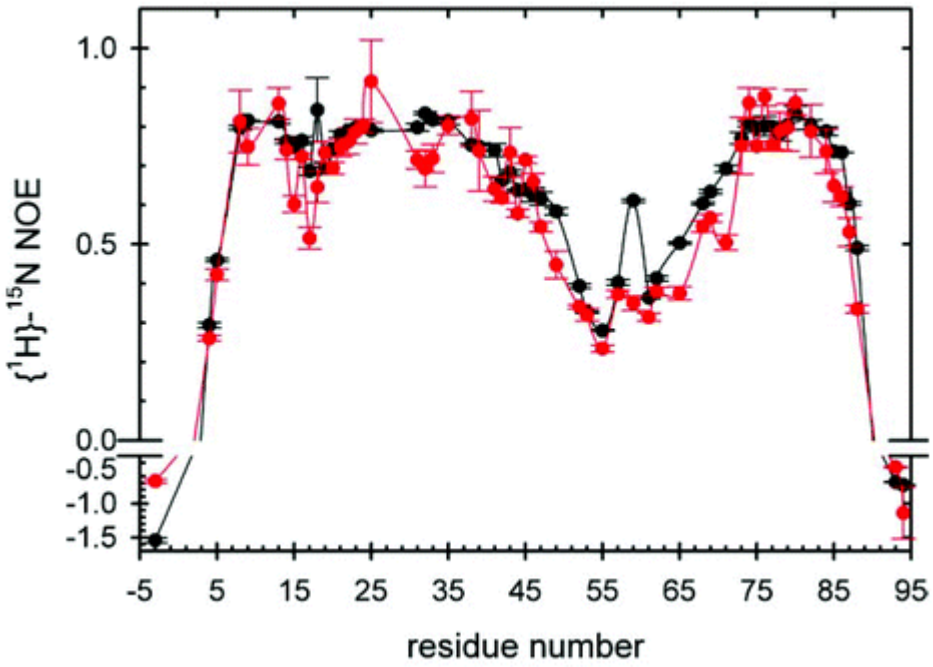

Fig. 2 Steady-state $\{^1\text{H}\}-^{15}\text{N}$ NOE values for apocytochrome b_5 residues quantified in cells (red) and in dilute solution (black) at 25 °C, 700 MHz. [14]

Interpreting small decreases in intracellular $\{^1\text{H}\}-^{15}\text{N}$ NOE values as increases in dynamics might be

appropriate under most circumstances. However, the $\{^1H\}-^{15}N$ NOE is affected by viscosity, which increases the correlation time by slowing the tumbling of the protein. The cytoplasm of *E. coli* has been shown to be slightly more viscous than dilute solution (water). With this in mind, most of the changes in apocytochrome b_5 backbone $\{^1H\}-^{15}N$ NOE values in cells are consistent with the 1.2 to 1.5-fold higher viscosity of the cytoplasm. [21]

Our investigation showed that quantitative information describing protein backbone dynamics can be obtained inside living cells, and that some of the observed differences track the change in viscosity rather than a change in fast backbone dynamics. Hence, it appears that the multitude of dilute solution steady-state $\{^1H\}-^{15}N$ NOE measurements already in the literature provide biologically relevant information about pico- to nanosecond backbone motion in proteins. [14]

More detailed dynamics

Likewise, in-cell protein NMR experiments were developed to measure the two other types of ^{15}N relaxation, longitudinal (T_1) and transverse (T_2) ^{15}N relaxation. [22] Once combined with the $\{^1H\}$-^{15}N NOE measurements, these data are used to evaluate the spectral density function at multiple frequencies. Spectral density analysis was performed to gain a more complete idea of the dynamics experienced by the protein backbone.

The spectral density function, $J(\omega)$, describes the distribution of the frequencies produced by a molecule's motion. The function can be thought of as the probability of finding a component of the molecule's motions at a specific frequency, ω. For fast motions the frequencies required for relaxation are similar to those that excite a spin (*i.e.*, the Larmor frequency). Eqn 1–3 describe a reduced set of linear combinations of frequency distributions required for ^{15}N relaxation [23]

$$J(0.87\omega_H) = \frac{1}{T_1}(NOE-1)\frac{\gamma_N}{\gamma_H}\frac{4}{5d^2} \quad (1)$$

$$J(\omega_N) = \frac{\left(\frac{1}{T_1}\right)-\left(J(0.87\omega_H)\left(\frac{7d^2}{4}\right)\right)}{\left(\frac{3d^2}{4}\right)+c^2} \quad (2)$$

$$J(0) = \frac{\left(\frac{1}{T_2}\right)-\left(J(\omega_N)\left(\frac{3d^2}{8}+\frac{c^2}{2}\right)\right)-\left(J(0.87\omega_H)\left(\frac{13d^2}{8}\right)\right)}{\left(\frac{d^2}{2}\right)+\left(\frac{2c^2}{3}\right)} \quad (3)$$

where, $c = \Delta\sigma\omega_N/\sqrt{3}$, $d = (\mu_0\gamma_H\gamma_N h/(8\pi^2))\langle r^{-3}_{NH}\rangle$, $\Delta\sigma$ is the chemical shift anisotropy (here, 160 ppm), μ_0 is the permeability of free space, γ_H and γ_N are the gyromagnetic ratios for ^1H and ^{15}N, h is Planck's constant, and r_{NH} is the internuclear ^1H–^{15}N distance (1.02 Å). Although not shown in the equation for $J(0)$, T_2 also depends on slower motion. Here I will only focus on fast (ps–ns) motions.

Reduced spectral density mapping, however, can be difficult to relate to the internal motions experienced by the protein backbone in addition to the overall tumbling of the protein. Lipari and Szabo [24,25] introduced a

'model-free' analysis that assumes a simple form for the spectral density function $J(\omega)$. The model-free analysis allows for the separation of the overall tumbling motion of the protein from internal motions and relates the spectral density to an order parameter, S^2, and an internal effective correlation time, τ_e:

$$J(\omega) = \frac{2}{5}\left[\frac{S^2\tau_m}{1+\omega^2\tau_m^2} + \frac{(1-S^2)\tau}{1+\omega^2\tau^2}\right] \quad (4)$$

where S^2 is the measure of spatial restriction of the internal motion, τ_e is the measure of the timescale of the internal motion, τ_m is the overall rotational correlation time for isotropic tumbling, and $1/\tau = (1/\tau_e) + (1/\tau_m)$. [24,25] The order parameter, S^2, indicates the amplitude of motion experienced by a ^1H–^{15}N spin-pair along the bond vector and has a range from 0 to 1, where 0 corresponds to no restriction of motion and 1 corresponds to full restriction or no motion.

We went one step farther in our analysis and used Lipari–Szabo mapping [26,27] which is a graphical method for analyzing spectral densities in terms of the Lipari–Szabo model-free analysis. [24,25] The two spectral densities, $J(0.87\,\omega_H)$ and $J(\omega_N)$, are determined and plotted against one another (Fig. 3). In addition, a general outline of a Lipari–Szabo map for a rigid molecule ($S^2 = 1$, $\tau_e = 0$) is plotted by determining $J(0.87\,\omega_H)$ and $J(\omega_N)$ values for a range of τ_m values using eqn 5.

$$J(\omega) = \frac{2\tau_m}{5(1+\omega^2\tau_m^2)} \quad (5)$$

where ω is the frequency of interest and τ_m is the correlation time. A resulting three-sided curve representing a range of different τ_m values is shown in Fig. 3 with the τ_m values indicated. The two lines in Fig. 3 show the effects of the various Lipari–Szabo parameter combinations with τ_m set to 5.5 ns (point of intersection), a reasonable value for apocytochrome b_5 in dilute solution. [16] The lower line represents values where τ_e was set to 0 and the tick marks, from right to left, show decreasing values of S^2, from 1 to 0.3, in increments of 0.1. Likewise, the upper line has a τ_e value set to 100 ps. In general, then, points move to the left when their amplitude of independent motion increases (decreasing S^2) and move up when their timescale of independent motion increases.

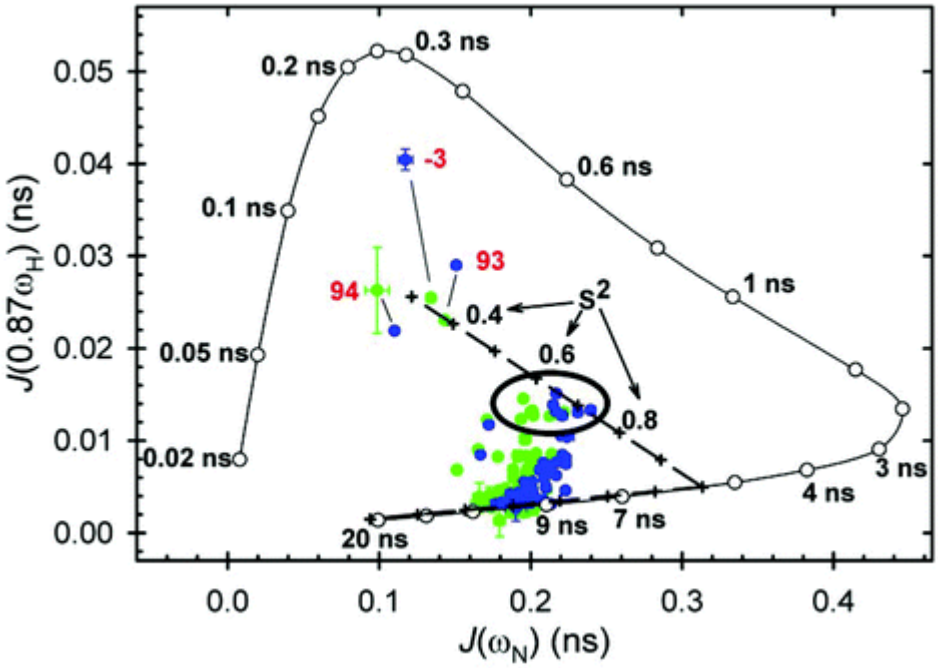

Fig. 3 Lipari–Szabo map comparing apocytochrome b_5 backbone dynamics in living *E. coli* (green) and in dilute solution (blue) (Bryant, Lecomte, Lee, Young and Pielak). The $J(0.87\,\omega_H)$ and $J(\omega_N)$ values for 56 apocytochrome b_5 residues were calculated from relaxation measurements acquired at 700 MHz, 25 °C. Each point is the average of three independent measurements and the vertical and horizontal bars indicate one standard error for $J(0.87\,\omega_H)$ and $J(\omega_N)$, respectively. Most of the uncertainties are smaller than the points. Selected residue numbers are shown in red, with connecting lines indicating the difference in location of the points in dilute solution and in cells. The three-sided curve represents the projected behavior for a hypothetical Lipari–Szabo rigid molecule with different values of τ_m, which are shown along the outside of the curve. The upper and lower dashed lines are from simulations where τ_m was set at 5.5 ns and τ_e was set at 0 (lower line) and 0.1 ns (upper line). The tick marks along the lines, from right to left, indicate S^2 values from 1.0 to 0.3 in increments of 0.1. The points located within the ellipse represent residues from the heme-binding loop.

Changes in cells

Complete data sets for 56 apocytochrome b_5 residues were obtained under both dilute solution and intracellular conditions. These data were analyzed using Lipari–Szabo mapping [26,27] and the results are shown in Fig. 3 where the in-cell data are shown in green and the dilute solution data in blue. Upon first glance, the most obvious conclusions that can be made about the data is that though they are similar in trend, the data from inside cells is shifted to the left of the data obtained in dilute solution.

To find regions whose dynamics are similar under both conditions, residues were identified for which

spectral-density pairs change by less than the sum of their uncertainties. Twenty-nine residues fit this criterion. Twenty of these residues occur in the more structured regions of the protein. There were 27 residues whose spectral densities in dilute solution and in cells change by more than the sum of their uncertainties. Thirteen of these residues are from the heme-binding loop and 8 are from the disordered N- and C-termini and the loop between residues 8 and 20.

Despite these differences, a more detailed analysis shows that the intracellular environment does not change the average S^2 value, amplitude of motion, for the residues (Fig. 4). On the other hand, there is an average increase in τ_e, the timescale of these independent motions, for the more structured regions and no change in the least structured regions of the protein (Fig. 4). Therefore, we concluded that the cytosol does not greatly affect the overall fast dynamics of apocytochrome b_5. [22] This analysis shows that the differences seen in the Lipari–Szabo map in Fig. 3 are most likely due to an increase in the viscosity of the cytosol.

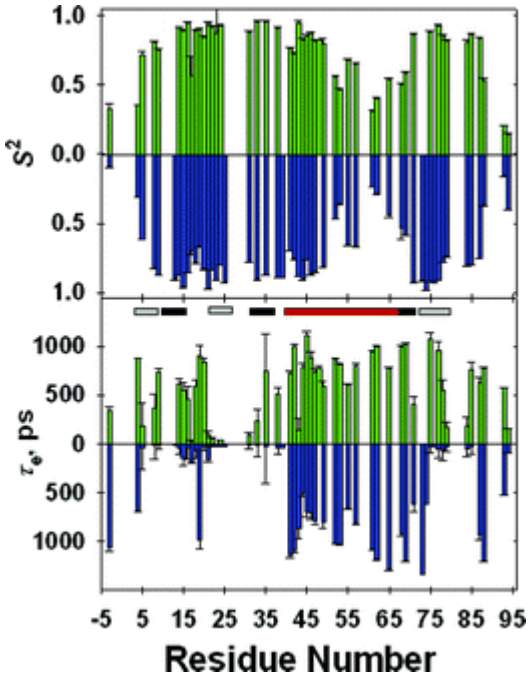

Fig. 4 Histograms of S^2, and τ_e with their uncertainties in dilute solution (blue, τ_m 9.6 ns) and in cells (green, τ_m 10.9 ns) from fitting the T_1, T_2 and NOE data. The numbering system is based on the sequence of bovine cytochrome b_5. Approximate regions of secondary structure [29] are shown below the top panel (β-strand; gray; α-helix, black; heme-binding loop, red).

Summary and prospective

We accomplished our aim to develop a technique that yields quantitative information and used it to investigate protein dynamics in living cells. In doing so, we found quantitative differences in the spectral densities of many residues along the backbone of apocytochrome b_5 inside cells compared to dilute solution. After further analysis, however, the cytosolic environment was found to have only a small effect on the timescale of fast backbone dynamics most likely explained by the increase in viscosity of the cytosol. The most important conclusion is that the intracellular environment does not affect the overall pattern of fast

backbone dynamics, validating dilute solution studies of protein dynamics. [22] Our work shows that future studies need to focus on the effects of viscosity on protein dynamics and that new studies should be directed to measuring the slower dynamics experienced by the protein backbone not discussed here.

Acknowledgements

I thank Juliette T. J. Lecomte, Andrew L. Lee, Gregory B. Young and especially my advisor Gary J. Pielak for all their help throughout this project.

References

1 K. Luby-Phelps, *Int. Rev. Cytol.*, 2000, **192**, 189–221 .
2 D. M. Hatters , A. P. Minton and G. J. Howlett, *J. Biol. Chem.*, 2002, **277**, 7824–7830 .
3 M. M. Dedmon , C. N. Patel , G. B. Young and G. J. Pielak, *Proc. Natl. Acad. Sci. U. S. A.*, 2002, **99**, 12681–12684 .
4 G. Rivas , J. A. Fernandez and A. P. Minton, *Proc. Natl. Acad. Sci. U. S. A.*, 2001, **98**, 3150–3155 .
5 K. Sasahara , P. McPhie and A. P. Minton, *J. Mol. Biol.*, 2003, **326**, 1227–1237 .
6 Z. Serber , R. Ledwidge , S. M. Miller and V. Dötsch, *J. Am. Chem. Soc.*, 2001, **123**, 8895–8901 .
7 Z. Serber , A. T. Keatinge-Clay , R. Ledwidge , A. E. Kelly , S. M. Miller and V. Dötsch, *J. Am. Chem. Soc.*, 2001, **123**, 2446–2447 .
8 Z. Serber and V. Dötsch, *Biochemistry*, 2001, **40**, 14317–14323 .
9 Z. Serber , W. Straub , L. Corsini , A. M. Nomura , N. Shimba , C. S. Craik , P. O. de Montellano and V. Dötsch, *J. Am. Chem. Soc.*, 2004, **126**, 7119–7125 .
10 Z. Serber , L. Corsini and V. Dötsch, *Methods Enzymol.*, 2005, **394**, 17–41 .
11 N. Shimba , Z. Serber , R. Ledwidge , S. M. Miller , C. S. Craik and V. Dötsch, *Biochemistry*, 2003, **42**, 9227–9234 .
12 B. C. McNulty , G. B. Young and G. J. Pielak, *J. Mol. Biol.*, 2005, **355**, 893–897 .
13 D. S. Burz , K. Dutta , D. Cowburn and A. Shekhtman, *Nat. Methods*, 2006, **3**, 91–93 .
14 J. E. Bryant , J. T. J. Lecomte , A. L. Lee , G. B. Young and G. J. Pielak, *Biochemistry*, 2005, **44**, 9275–9279 .
15 J. A. Hubbard , L. K. MacLachlan , G. W. King , J. J. Jones and A. P. Fosberry, *Mol. Microbiol.*, 2003, **49**, 1191–1200 .
16 S. Bhattacharya , C. J. Falzone and J. T. Lecomte, *Biochemistry*, 1999, **38**, 2577–2589 .
17 A. J. Constans , M. R. Mayer , S. F. Sukits and J. T. Lecomte, *Protein Sci.*, 1998, **7**, 1983–1993 .
18 W. Pfiel, *Protein Sci.*, 1993, **2**, 1497–1501 .
19 K. Lindorff-Larsen , R. B. Best , M. A. Depristo , C. M. Dobson and M. Vendruscolo, *Nature*, 2005, **433**, 128–132 .
20 L. E. Kay , D. A. Torchia and A. Bax, *Biochemistry*, 1989, **28**, 8972–8979 .
21 S. Bicknese , N. Periasamy , S. B. Shohet and A. S. Verkman, *Biophys. J.*, 1993, **65**, 1272–1282 .
22 J. E. Bryant , T. J. Lecomte , A. L. Lee , G. B. Young and G. J. Pielak, *Biochemistry*, 2006 , in press.
23 A. G. Palmer, *Annu. Rev. Biophys. Biomol. Struct.*, 2001, **30**, 129–155 .
24 G. Lipari and A. Szabo, *J. Am. Chem. Soc.*, 1982, **104**, 4546–4559 .
25 G. Lipari and A. Szabo, *J. Am. Chem. Soc.*, 1982, **104**, 4559–4570 .
26 M. Andrec , G. T. Montelione and R. M. Levy, *J. Biomol. NMR*, 2000, **18**, 83–100 .
27 W. M. Hanson , S. A. Beeser , T. G. Oas and D. P. Goldengerg, *J. Mol. Biol.*, 2003, **333**, 425–441 .
28 A. P. Minton, *J. Biol. Chem.*, 2001, **276**, 10577–10580 .
29 C. J. Falzone , M. R. Mayer , E. L. Whiteman , C. D. Moore and J. T. J. Lecomte, *Biochemistry*, 1996, **35**, 6519–6526 .

Footnote

† Current address: Schering-Plough Corporation, Kenilworth, NJ 07033, USA, Email: bryant.je@gmail.com, Tel.

(908) 740-3425.

2006